SYNTHESIS AND CHARACTERIZATION OF MAGNETIC NANO FERRIC OXIDE COAGULANT

Dr. Kalam Narren, Dr. Vinay Kumar[1], Dr. Dhinesh Kumar[1], Dr. Winston Dunn [1*]

1*Assistant professor, PG and Research Department of Chemistry, G. T. N Arts College (Autonomous), Old karur road, Dindigul-624005.

ABSTRACT

Pure water is essential for survived of human being. To meet the requirement of potable and domestic water, the immediate need is to treat the waste water. These effluents are highly harmful and unsafe. The removal of contaminated is must in reuse. The treatment process included the process of coagulation, flocculation and absorption, in modern days some magnetic nano particles are used to treat the effluent. The main purpose of this project is to enhance the effectivity of nano Ferric Oxide Coagulant

INTRODUCTION

Nanotechnology is a field of applied science focused on the design, synthesis, characterization and application of materials and devices on the nano scale. Nanotechnology relying on the manipulation, control and integration of atoms and molecules to form materials, structure, components, devices, and systems at the nano scale, is the application of nanoscience, especially to industrial and commercial objectives. In particular that nanotechnology consists of materials with small dimension, remarkable properties, and great application potential

Nanotechnology is an identified field of research since last century. Since “nanotechnology” was presented by Nobel laureate Richard P.Feyn- man during his well famous 1959 lecture “Theres plenty of room at the Bottom” (1-6) there have been made various revolutionary development in the field of nanotechnology. Nanotechnology produced materials of various types’ ai nanoscale level. Nanoparticles are wide class of materials that include particulate substance, which have one dimension less than 100nm at least (3,4), and can be termed as a nanoparticles.

Nanotechnology (1,2) refers to the exacting scientific purpose of precisely manipulating atoms and molecules for the fabrication of macro scale products, with a radius less than 100 nm can be termed as a nanoparticles. They can be including fullerence, metal clusters, large molecule, such as protein and hydrogen bonded assemblies of water moleculer.

Nanotechnologies are now widely measured to have the potential to bring benefits in areas as various as drug development, water decontamination, information and communication technologies, and the production of stronger and lighter materials. Nanotechnologies occupy the manufacture and manipulation of materials at the nanometer scale, either by scaling up from single groups of atoms or by refining or reducing bulk materials [3].

Now day's nanotechnology has been one of the most important and exciting fields in physics, chemistry .engineering and medicine. The field of nanotechnology is a promising one provides us with many breakthroughs that will alter the direction of technological advance in a variety of application. The first observation was that materials can be nanostructures for few and novel performance.

The particles which are smaller than the characteristic length display new chemistry and physics, leading to the new behavior which depends on the size. For example, the mechanical properties, conductivity and reactivity have been observed to vary when particles become smaller then a critical size.

Synthesis of Gamma Ferric Oxide (γ-Fe2O3)

In the present study, ferrous oxalate used as a precursor. Thermal decomposition of Iron Oxalate precursor was done by employing Polyethylene glycol (PEG) as a surface modifying agent. In the present process, a stainless steel bowl shaped container was used. The ferrous oxalate was taken and mixed with PEG in the ratio of 1:5. The container was given heat treatment, the reaction mixture burned initially with an oxidizing flame which then converts to reducing flame and leads to formation of final residue. The flame once got ignited leads to the formation of high surface γ-Fe2O3 as residue(6-9). The whole reaction is completed within 10 minutes. On cooling to room temperature, no traces of carbon impurities were observed in the final residue of γ-Fe2O3. The highest temperature of the reaction was found to be around 500^{o}C.

Synthesis of Ti doped with Gamma Ferric Oxide (γ-Fe2O3)

To prepare doping material, the following solutions were used. Fixed concentration of TiO2 (0.001mol/L) and Fe2O3 (0.1mol/L) was used. The solution of Fe2O3 was taken in a beaker then 30 ml of TiO2 solution added to it at 100oC for 2 hours in the ratio of 0.1ml/min, after two hours the color changed from dark brown to blood red color(12-16), indicating the formation of product. The product is washed with water and 0.01N HNO3. Then it was dried in 120oC for half an hour and then calcinated at 6500C for 1-2hrs to get a fine powder.

X-RAY DIFFRACTION

XRD is used to confirm the inorganic sample through its crystal structure and lattice parameter. XRD pattern of sample is shown in the Fig-(1,2) the sharp peak of XRD at 23.576 2θ and 41.821 2θ shows the samples have highly crystal nature, and the multi-peaks at 33.041 2θ and 33.714 2θ shows that the doping exists in the sample γ-Fe_2O_3 doped with Ti (S Riyas et al.). All the peaks are matched with the standard JCPDS Card No. 89-2811 of trigonal (rhombohedral) structure of calcium hydroxide. The additional peaks present in the XRD data is within the allowable 3% detection limit of commercial XRD (G. Taglieri. et al.) Hence the impurity level in the synthesized sample may be highly negligible. To Further prove the size of the Fe_2O_3 doped with Ti, studied the cell parameter values, which one was compared with JCPDS and run the Diamond 4 software by using the raw data XRD file. This data is shown in the Table-1 the cell parameter of γ-Fe_2O_3changed to a=b=5. 0316 and c=13. 8030 Å from a=b=c=3.860Å due to doping. Normally the gamma Iron Oxide shows the cubic structure, but it shows that the Trigonal (Rhombohedral) structure and cell parameter also changed. Doping implies that the added metal is incorporated into the crystal structure of the host rather than forming side phases (Henrique. J et al.). The dopant will affect the structure by expanding or contracting it based on the size differences and bonding (valence) differences, or possibly change the symmetry.

The peak at 25.576Å (012), 33.041 (104) and 33.714 (110) were the confirmation peak for Fe_2O_3 doped with Ti. The peaks at 33.041 (104) and 33.714 (110) shows overlap. This one may indicate the doping of Titanium. (Fu Su Yen et al.). The peak at 41.196 (400) represents to the Ti. The lattice parameter shows the change in morphology. The space group of the sample also changed from P4332 to $R\bar{3}$ because the Fe (II) and Ti (IV) are penetration,. Into their respective site. However, we find Fe and Ti at both cation sites, indicating a trend towards an $R\bar{3}$ structure. Fe (II) and Ti (IV) are octahedrally coordinated by oxygen and penetration into layers. Inside the layers, each cation has three immediate neighbors, and across layers it has one neighbor. The coordination O (II) -octahedra around Fe (II) and Ti (IV) in neighboring layers are sharing either faces or corners, while within layers, the octahedra are sharing edges. Although these data provide evidence about the homogeneity of the solid solutions, the refinement of the x-ray diffraction patterns cannot deliver information about the internal crystal structure.

Table-1 Lattice parameter of sample for γ-Fe_2O_3 doped with Ti

Cell parameter	γ-Fe_2O_3	γ-Fe_2O_3 doped with Ti
A	3.860	5.0316
B	3.860	5.0316
C	3.860	13.8030

Table-2 2θ values and hkl values for γ-Fe_2O_3 doped with Ti

Angle 2 Theta °	γ-Fe_2O_3 hkl value	γ-Fe_2O_3 doped with Ti hkl value
23.576	220	012
33.041	104	104
33.714	311	110
41.176	021	400
41.821	202	422

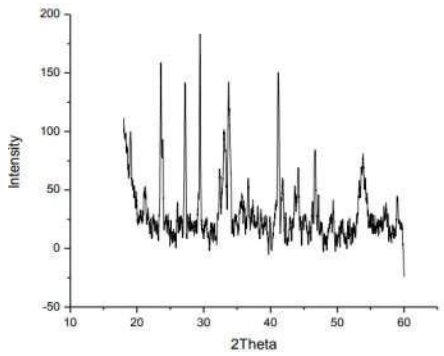

Fig-1 X-ray diffraction pattern for sample γ-Fe2O3 doped with Ti

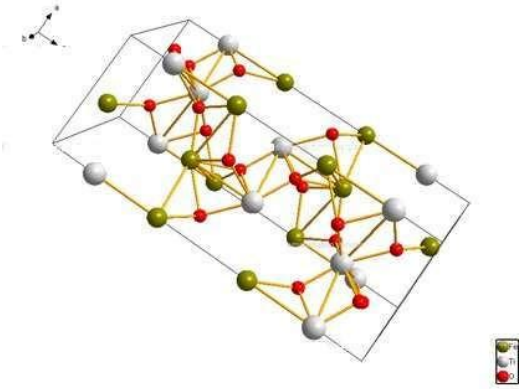

Fig-2 The atomic arrangement of the nano particle. Image draw by using Diamond-4

SCANNING ELECTRON MICROSCOPE

The scanning electron microscope is used to find the shape and size of the nano particle. From the image it is clear that the particle shape changed from spherical to needle shape. Because, the doping changed the lattice arrangement to Trigonal (Rhombohedral) from cubic. In Ti atoms, atomic radius is lesser than Fe, atomic radius it affects the shape. The histogram graph shows the particles are not equally distributed and the size varies from 20-70 nanometers. This due to the environmental factors like room temperature, atmospheric air moisture etc.

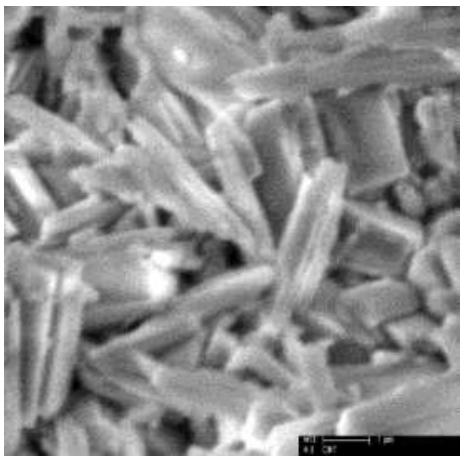

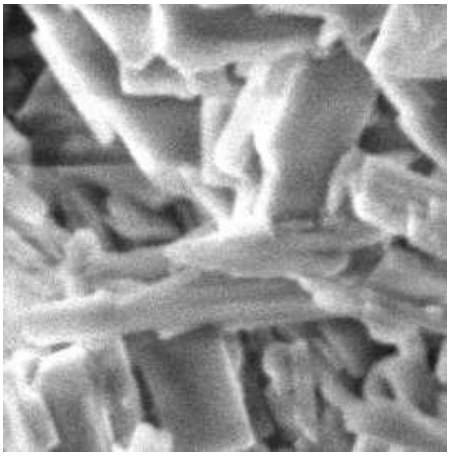

Fig-3, 4 represent for the SEM image of γ-Fe_2O_3 doped with Ti

Effect of temperature

When the temperature increased, the volume of the liquor would expand and resulting in a reduction of supersaturation, which diminished the nucleation rate and promoted the growth rate of the particles (Chia Chin Hua et al). When the preparation temperature of doped material

was maintained at 1200C, the constant temperature gives an equal arrangement of the lattice and particles are formed less than 100 nm.

Effect of doping

When the doping takes place the impurity added to the parent material due to the impurity, the lattice arrangement of the parent material changed. When add a known impurity to parent material, the lattice disorder takes place on it due to lattice disorder. Hence the morphology of the parent material was changed (Michalis Charilaou et al., MilanCekerevac et al.). In the present study, Ti used as a doping material and γ-Fe2O3 was used as the parent material. Atomic radius of Fe is higher than Ti, so the doping takes place in good manner. The lower atomic radius gives best result in a doping and from lattice disorder this lattice disorder gives change in morphology (Nedelec. J. M et al).

FTIR

The sample shows absorption in the range of 466 cm-1, 793.94 cm-1, 825.07 cm-1, 892.95 cm-1, 1382.86 cm-1, 1624.95 cm-1, 1761.63, 2393.54 cm-1, and 3218.84 cm-1, 3778.13cm-1. The general range of 1800-2100 cm-1 may assign for transition metal,Observed in a region of 3218 and 1624 cm–1are indicated as hydrates, 1670–1600 cm–1 (relating to OH bending). The peaks in the range between 722-3111cm-1and 722-2924cm -1shows the presence of Fe2O3 and Ti in the sample. 466 and 579cm-1Specific bending vibrations of Fe-O bond (Ning Du et al.). 793cm-1 assigned to the vibrations of Ti–O and Ti–O–Ti framework bonds.

Table-3 FTIR assignment for γ-Fe2O3 doped with Ti

Wave Length	Function Group
328 and 1624 cm-1	Hydrates
1800-2100 cm-1	Transition metal
1624–1600 cm-1	OH bending
793 cm-1	Assigned to the vibrations Of Ti–O and Ti–O–Ti framework bonds
579 cm-1	Specific bending vibrations of Fe- O bonds
466 cm-1	Specific bending vibrations of Fe- O bonds

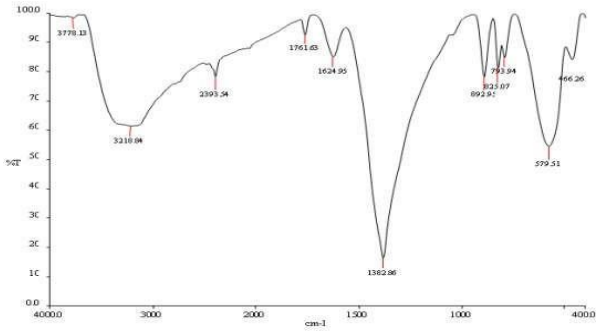

Fig-5 FTIR spectrum of the doped γ-Fe2O3

SUMMERY AND CONCLUSION

γ-Fe_2O_3 nano particle was prepared by self-propagation method and doped with Ti The prepared γ-Fe_2O_3 doped with Ti is characterized by XRD, SEM, FTIR, From the XRD analysis, it is concluded that the doping with Ti and Mg replaced one Fe^{+2} ion in the peak 33.714 (311) and 59.596 (511) respectively. This replacement makes a crystal defect and the structure changed to trigonal from cubic for Ti doped When it doped with Ti, the lattice parameter changed to a=b=5. 0316 Å and c=13. 8.30 Å from a=b=c=3. 860Å it shows that the structural changes take place. But for Mg doped particle, there are no structural changes taking place. The sample remains in cubic structure, but the lattice parameter changed to a=b=c=8.366Å from a=b=c=3.86Å. From the above lattice parameter calculations, it is concluded that doping increased the lattice parameter; the increased lattice parameter gives bigger size grains and bigger size particles. From SEM analysis, it concluded that the samples are formed in 60-75nm and shows needle shape morphology for Ti doped Fe_2O_3. From FTIR it concluded that the absorption at 1800-2100cm-1 assigned for transition metal. The absorption at 1670-1600cm-1 assigned for OH bending. The absorption at 579cm-1 and 466cm-1assigned for Specific bending vibrations of Fe-O bonds. The absorption at 793cm-1 assigned for the vibrations of Ti–O and Ti– O–Ti framework bonds. The prepared nano-coagulant is used for water treatment in future studies

REFERENCE

1. Pandiarajan, A., Shanmugaselvan, R., & Dheenadayalan, M. S. (2023). ENVIRONMENTAL SCIENCE ARCHIVES. Environmental Science, 2(1), 59.
2. P. U. Mageshwari, J. Jayarubi, A. U. Sundari, S. Sundaranayagi, R. Anandhi and R. S. Selvan, Educational Administration: Theory and Practice, 30(4), 7008(2024),

https://doi.org/10.53555/kuey.v30i4.2506

3. 20. S. Sulochana, K. Soundaravalli and R. S. Selvan, Oriental Journal of Chemistry, 38(3), (2022), http://dx.doi.org/10.13005/ojc/380310
4. Selvan, R. S., & Gokulakrishnan, K. (2013). Preparation and Characterization of Mg Doped γ-Fe2o3 Prepared by Self-Propagation Method. International Journal of Applied Chemistry, 9(3), 291-297.
5. Mageshwari, P. U., Jayarubi, J., Sundari, A. U., Sundaranayagi, S., Anandhi, R., & Selvan, R. S. (2024). Synthesis, And Characterization Of Metal Oxide (Cuo) Nanoparticles By Simple Precipitation Method. Educational Administration: Theory and Practice, 30(4), 7008-7012.
6. Selvan, R. S., & Gokulakrishnan, K. (2017). Effect of Doping in Magnetic Character in γ-Fe2O3 Nano Particle.
7. Roman Boulatov, Nature Chemistry, 13,112(2021), https://doi.org/10.1038/s41557-020-00623-9
8. Mohammad Amin Alavi and Ali Morsali, Journal of Experimental Nanoscience, 5(2), 93(2010), https://doi.org/10.1080/17458080903305616
9. Zhengxin Guan a, Liqiang Liu b, Xiyan Xu a, Acan Liu a, Han Wu a, Jun Li b, Wei Ou-Yang aNano Energy, 104(Part A), 107879(2022), https://doi.org/10.1016/j.nanoen.2022.107879
10. S. Lempri`ere, Nature Reviews Neurology,19, 326(2023), https://doi.org/10.1038/s41582-023-00816-z
11. Rodrigo Araya-Hermosilla, Jessica Martínez, C´esar Zúniga ˜ Loyola, Sara Ramírez, Sebastian ´Salazar, Charles S. Henry, Roberto Lavín, Nataly Silva, Ultrasonics Sonochemistry, 99, 106545(2023), https://doi.org/10.1016/j.ultsonch.2023.106545
12. B. Ling, J. Lee, D. Maresca, A. Lee-Gosselin, D. Malounda, M.B. Swift, M. G. Shapiro, ACS Nano, 14(9),12210(2020), https://doi.org/10.1021/acsnano.0c05912
13. C Nolla-Colomer, C Tarifa, A Llach, V Jimenez-Sabado, A Vallmitjana, S Casabella, H Colino, P Izquierdo, S Casellas, E Rodriguez-Font, J Cinca, S.R.W Chen, R Benitez, L Hove-Madsen, European Heart Journal, 41(2), 3689(2020), https://doi.org/10.1093/ehjci/ehaa946.3689

14. D.P. Sawyer, A. Bar-Zion, A. Farhadi, S. Shivaei, B. Ling, A. Lee-Gosselin, M. G. Shapiro, Nature Methods, 18, 945(2021), https://doi.org/10.1038/s41592-021-01229-w
15. C. Wang, X. Chen, L. Wang, M. Makihata, H.-C. Liu, T. Zhou, X. Zhao, Science, 8(42), 517(2022), https://doi.org/10.1126/science.abo2542
16. P. Qin, K. Wu, Y. Hu, J. Zeng, X. Chai, IEEE Journal of Biomedical and Health Informatics, 24,1028(2020), https://doi.org/10.1109/jbhi.2019.2950994